

Effective MagnetoElectric Properties of MagnetoElectroElastic (Multiferroic) Materials and Effects on Plane Wave Dynamics

Scott M. Keller^{*}, Abdon E. Sepulveda, and Gregory P. Carman

Abstract—In this paper we analyze the 3D modes of a linear homogeneous magneto-electroelastic (MEE) material reduced to magneto-electric (ME) constitutive form. This allows convenient examination of the predominately electromagnetic behavior in a mechanically coupled MEE material system. We find that the behavior of the electromagnetic modes are strongly influenced by the mechanical coupling present in the MEE material system. A number of papers refer to the cross-coupling of laminated piezoelectric and piezomagnetic materials as magneto-electric materials. We discuss here that the composite materials are MEE systems and that the constitutive relations need to reflect the mechanical coupling also. Further, we find that the mechanical coupling has a significant impact on the electromagnetic propagation modes of the composite material. Through examples of homogenized MEE materials we show possibilities for remarkable electromagnetic material characteristics which are not conventionally obtainable in single phase materials.

1. INTRODUCTION

Historically, magneto-electric (ME) materials were nothing more than a scientific curiosity. In the 1950's and 60's, research on single phase materials proved both the existence of ME materials [1] and that single crystal materials are inadequate for most engineering applications, since the cross-coupling effect was generally too weak to be of practical value [2,3]. The development of composite materials, however, has produced orders of magnitude increase in the strength of magneto-electric coupling effects [4]. New curiosity has been generated in these unique materials over the past decade, with interest in applications such as magnetometers, phase shifters [5], Radar Absorbing Materials (RAM) and microwave devices [3,6], to mention a few. While initial research has focused largely on low frequency and static type applications, there has been growing interest in higher frequency applications. These high frequency applications require a solid understanding of wave propagation in these materials in order to determine how best to apply and design them.

Our primary interest here is understanding the electromagnetic (EM) wave behavior of ME materials. In most ME candidate materials the ME effect is produced through strain-coupling of a ferroelastic-ferroelectric phase with a magnetoelastic phase [6,7] (for example, bonding together thin layers of piezoelectric and piezomagnetic films). Under an applied electric field, the strain produced in the ferroelectric phase causes the material to strain (ferroelastic response). This strain is then transferred through mechanical bonding to the ferromagnetic phase, producing a change in the magnetization of the ferromagnetic material thru magnetoelastic effects. This is a product ME effect. When the magneto-electric effect is produced through strain-coupling, however, the constitutive relations for the materials are no longer strictly ME but now have additional mechanical coupling. Consequently, to understand the EM wave propagation in these materials, the wave behavior of the multi-physics

Received 20 August 2015, Accepted 1 November 2015, Scheduled 18 December 2015

^{*} Corresponding author: Scott M. Keller (smkeller@ucla.edu).

The authors are with the Department of Mechanical and Aerospace Engineering, University of California, Los Angeles, California 90095, USA.

coupling of the composite must be understood. In modeling this response, it is computationally more efficient to treat the composite material as a homogeneous mixture rather than separate ferroelectric and ferromagnetic phases. This assumption is reasonable for wavelengths substantially greater than the dimensions of individual phases in the composite material. These homogenized models are not strictly magnetoelectric anymore but also have direct coupling with mechanical fields. The resultant constitutive relations being magnetoelastoelectric (MEE). Thus, the problem of understanding wave propagation in strain-coupled ME materials is actually the problem of understanding wave propagation in MEE materials.

While MEE materials have been studied for quite some time, there are surprisingly few papers on wave propagation in MEE materials. Earlier works, such as Wang [21], recognize the need to treat homogenous composite materials as MEE materials and produced models to predict the aggregate behavior. Other authors [15, 16] have modeled the magnetoelectric cross-coupling properties of two phase composite systems but were not focused on general models of MEE coupling. Experimental efforts have verified the effectiveness of strain coupled materials [18, 20] for static application and the materials community is starting to exam strain coupled materials for high frequency electromagnetic wave applications [17, 19]. Chen [8] did work on reflection and transmission coefficients in MEE materials in the quasi-static limit, while Iadonisi [9], published a paper on wave propagation for specific material symmetries with full dynamics included, though only considering propagation along crystal axes. Yang [10] and Pang [12] has worked on magnetoelastoelectric wave propagation in materials with equations of mechanical dynamics but with the limiting assumption of electrostatics. Chen [13] considers interface effects in multilayered plates and considers the field variable continuity conditions across the interfaces. Bin [14] presents the dynamic solution for MEE plates composed of magnetostrictive and piezoelectric layers. All of these authors have focused on the predominately acoustic modes of wave propagation and generally in the quasistatic limit.

No one has yet looked at the treatment of MEE materials from the viewpoint of extracting the magnetoelectric material properties and the influence of *mechanical* effects on electromagnetic behavior. The focus of the present paper is to examine fully dynamic electromagnetic wave propagation in MEE materials and illustrate how dramatically the mechanical coupling can influence the EM wave propagation. A new approach that incorporates the full physics of the MEE material system and then reduces the system of equations to an ME system with new “effective” properties is proposed. Relevant examples comparing EM wave modes with and without mechanical effects are presented to highlight the importance of including the material stiffness in analysis.

2. BACKGROUND

ME materials exhibit cross-coupling between the magnetic and electric fields such that an electric field can induce magnetization and, similarly, a magnetic field can induce polarization in the material. Assuming linear response, the constitutive relations that capture this behavior contain cross terms in the electric flux density (displacement field), \bar{D} , and the magnetic flux density (magnetic induction), \bar{B} such that

$$\bar{D} = \bar{\epsilon}\bar{E} + \bar{\xi}\bar{H} \quad \text{and} \quad \bar{B} = \bar{\xi}^T \bar{E} + \bar{\mu}\bar{H} \quad (1)$$

where \bar{E} and \bar{H} are the electric and magnetic fields. Plane wave solutions to Maxwell’s Equations combined with the above constitutive form produce two modes of propagation and two, possibly degenerate, phase velocities for each direction of propagation. In conventional isotropic materials, these modes are electrically and magnetically polarized perpendicular to the direction of wave propagation and are often referred to as the transverse electric and transverse magnetic modes. Furthermore, in isotropic materials the phase velocity does not depend on direction, while in anisotropic and cross-coupled materials, this is usually not the case. The electric and magnetic fields are no longer assured to be transverse or mutually perpendicular, and the velocities and modes vary with the direction of propagation.

Similarly, if we consider a purely mechanical system with linear constitutive relations of the form $\bar{S} = \bar{s}\bar{T}$ where \bar{S} is the strain, \bar{T} the stress and \bar{s} the compliance tensor in Voigt notation, then, plane wave solutions of this system yield three acoustic modes with possibly degenerate phase velocities: two

corresponding to shear modes, and the third to a longitudinal wave along the direction of the wave vector. As with general electromagnetic materials, the velocities and modes for mechanical propagation vary with direction in the material.

For MEE materials, it is necessary to combine the equations of motion for both electromagnetic and mechanical degrees of freedom. In general, MEE materials will have five modes of propagation and five different phase velocities in each direction. The five modes are not directly the acoustic plus electromagnetic modes that one would obtain if considering the mechanical properties (stiffness/compliance tensor) and electromagnetic properties (permittivity and permeability) separately. Rather, the coupling of the mechanical and electromagnetic properties through piezoelectric and piezomagnetic phenomena cause a hybridizing of the “base” modes of the system, causing a shift in the phase velocities and “mixing” of eigenmodes of the system, depending of course upon the particular combination of material parameters associated with the system. In the MEE system, we can think of the modified acoustic modes as “primarily acoustic” and the electromagnetic modes as “primarily electromagnetic”.

3. ANALYSIS

3.1. Reduced Constitutive Form

In the following section, constitutive relations for a general linear lossless MEE system are presented. The equations of elastodynamics are used to reduce the constitutive form to an effective magnetoelectric material form which can then be used for the solution of EM waves in a magnetoelectric material. For a general lossless homogeneous linear magnetoelastoelectric material the constitutive equations are represented by

$$\bar{S} = \bar{s}\bar{T} + \bar{d}^T \bar{E} + \bar{q}^T \bar{H} \quad (2)$$

$$\bar{D} = \bar{d}\bar{T} + \bar{\epsilon}\bar{E} + \bar{\xi}\bar{H} \quad (3)$$

$$\bar{B} = \bar{q}\bar{T} + \bar{\xi}^T \bar{E} + \bar{\mu}\bar{H}. \quad (4)$$

The tensors \bar{s} , \bar{d} and \bar{q} are the compliance, piezoelectric and piezomagnetic material properties while $\bar{\epsilon}$, $\bar{\mu}$ and $\bar{\xi}$ are the permittivity, permeability, and magnetoelectric coupling parameters of the material. \bar{S} , \bar{T} , \bar{E} , \bar{H} , \bar{D} and \bar{B} are the strain, stress, electric, magnetic, electric displacement and magnetic induction fields. It should be noted that in the above equations, stress and strain fields, along with piezoelectric and piezomagnetic coupling coefficients are represented in Voigt notation. The particular ordering used for the Voigt “vector” forms is shown in Equation (11). For clarity, \bar{T} is used for stress in Voigt notation while $\bar{\bar{T}}$ would indicate the rank two stress tensor. Similar notation is used to distinguish strain while piezomagnetic and piezoelectric parameters are represented in Voigt “matrix” form throughout.

Our interest here is on the electromagnetic material parameters; the mechanical properties may seem incidental. However, as we show in this article, ignoring the non-magnetoelectric parameters (stress and strain) produces results which are different from those which include these parameters. This result is in sharp contrast to previous approaches which assume solutions are mechanically decoupled. Consequently, it is inappropriate to ignore the effects of the mechanical coupling on the electromagnetic wave modes. In what follows, we use the equations of mechanical equilibrium and small deformation in the strain constitutive relation (2), to account for the induced stresses and strains and then “eliminate” the stress dependence from the constitutive relations for electric displacement and magnetic induction fields. This provides a general framework that may be used to solve the mechanical equilibrium and Maxwell’s Equations for the phase velocities of traveling waves and the associated electric/magnetic field vectors.

The equations of motion for a mechanical system without body loads and small strains are

$$\nabla \cdot \bar{\bar{T}} = \rho \ddot{\bar{u}} \quad \bar{\bar{S}} = \frac{1}{2} (\nabla \bar{u} + \nabla \bar{u}^T) \quad (5)$$

where \bar{u} is the displacement vector and ρ is the material density. The source free Maxwell's Equations are

$$\begin{aligned}\nabla \times \bar{E} &= -\dot{\bar{B}} & \nabla \times \bar{H} &= \dot{\bar{D}} \\ \nabla \cdot \bar{D} &= 0 & \nabla \cdot \bar{B} &= 0\end{aligned}\quad (6)$$

For plane wave solutions in linear homogeneous media, the field quantities assume the form

$$\bar{Z}(\bar{x}, t) = \bar{Z} e^{i(k\hat{p}\cdot\bar{x} - \omega t)}, \quad (7)$$

where \bar{Z} represents one of the fields, and the wavevector is $\bar{k} = k\hat{p}$ where $\hat{p} = (\alpha_1, \alpha_2, \alpha_3)$ defines a unit vector in the propagation direction[†] and the α_i are direction cosines. Substituting (7) into Equations (5) and (6), the resultant equations in reciprocal space become

$$-i \frac{k}{\rho\omega^2} \hat{p} \cdot \bar{T} = \bar{u} \quad \bar{S} = i \frac{k}{2} (\hat{p} : \bar{u} + \bar{u} : \hat{p}) \quad (8)$$

$$\begin{aligned}\frac{1}{c} \hat{p} \times \bar{E} &= \bar{B} & \frac{1}{c} \hat{p} \times \bar{H} &= -\bar{D} \\ \hat{p} \cdot \bar{B} &= 0 & \hat{p} \cdot \bar{D} &= 0\end{aligned}\quad (9)$$

where $c = \frac{\omega}{k}$ is the phase velocity of the wave, and $\hat{p} : \bar{u}$ is the direct product of \hat{p} and \bar{u} .

From Equation (8) we see that the displacement \bar{u} is linear in the stress components and likewise the strains are linear in the displacements. For plane wave (harmonic) solutions this prompts us to rewrite the equations in (8) as matrix equations in terms of the Voigt vectors for stress and strain as follows:

$$\bar{u} = -i \frac{k}{\rho\omega^2} \bar{N} \bar{T} \quad \bar{S} = ik \bar{N}^T \bar{u} \quad (10)$$

where the "vectors" for stress, \bar{T} , strain, \bar{S} , the displacement vector, \bar{u} and direction operator matrix \bar{N} are expanded as

$$\bar{T} = \begin{bmatrix} T_{11} \\ T_{22} \\ T_{33} \\ T_{23} \\ T_{13} \\ T_{12} \end{bmatrix} \quad \bar{S} = \begin{bmatrix} S_{11} \\ S_{22} \\ S_{33} \\ 2S_{23} \\ 2S_{13} \\ 2S_{12} \end{bmatrix} \quad \bar{N} = \begin{bmatrix} \alpha_1 & 0 & 0 & 0 & \alpha_3 & \alpha_2 \\ 0 & \alpha_2 & 0 & \alpha_3 & 0 & \alpha_1 \\ 0 & 0 & \alpha_3 & \alpha_2 & \alpha_1 & 0 \end{bmatrix} \quad \bar{u} = \begin{bmatrix} u_1 \\ u_2 \\ u_3 \end{bmatrix}. \quad (11)$$

Combining the elastodynamics and small strain Equations (8) in Equation (10) leads to

$$\bar{S} = \frac{1}{\rho c^2} \bar{N}^T \bar{N} \bar{T}. \quad (12)$$

Using (12) to replace \bar{S} in (2) and rearranging

$$\left(\frac{1}{\rho c^2} \bar{N}^T \bar{N} - \bar{s} \right) \bar{T} = \bar{d}^T \bar{E} + \bar{q}^T \bar{H} \quad (13)$$

Defining $\bar{L} = \left(\frac{1}{\rho c^2} \bar{N}^T \bar{N} - \bar{s} \right)$ and assuming \bar{L}^{-1} exists, leads to

$$\bar{T} = \bar{L}^{-1} \bar{d}^T \bar{E} + \bar{L}^{-1} \bar{q}^T \bar{H} \quad (14)$$

which when substituted into Equations (3) and (4) produces

$$\bar{D} = \left(\bar{\epsilon} + \bar{d} \bar{L}^{-1} \bar{d}^T \right) \bar{E} + \left(\bar{\xi} + \bar{d} \bar{L}^{-1} \bar{q}^T \right) \bar{H} \quad (15)$$

$$\bar{B} = \left(\bar{\xi} + \bar{d} \bar{L}^{-1} \bar{q}^T \right)^T \bar{E} + \left(\bar{\mu} + \bar{q} \bar{L}^{-1} \bar{q}^T \right) \bar{H}. \quad (16)$$

[†] A more general formulation for non-homogeneous waves would allow \hat{p} to be complex. The current approach still applies but introduces additional complexity that is not needed for the types of materials analyzed in the present work, and so is not considered here. The assumption that $\bar{k} = k\hat{p}$ is fine for lossless materials, or at least systems with hermitian κ and ν matrices.

This provides the effective electromagnetic constitutive relations for a material with elastic coupling. For the purely ME system, direct analytic solutions for the phase velocities of the material are possible. The solution of the electromagnetic problem for a magnetoelectrically coupled material was addressed by the authors in a previous paper [11].

3.2. The Meaning of $\overline{\overline{L}}$

The above derivation of effective magnetoelastic constitutive parameters, Equations (15) and (16) relies on the invertibility of the 6×6 matrix $\overline{\overline{L}}$. It will be seen below that the $\overline{\overline{L}}$ matrix is invertible except for phase velocities, i.e., c values, corresponding to acoustic modes of the system.

In the previous section the calculation of the inverse of L was discussed under the assumption that L^{-1} exists. Here we would like to briefly discuss what is meant when this is not the case. Ultimately, this indicates that the phase velocity or eigenvalue found for the problem is identical to the acoustic eigenvalue and indicates that the stress (or traction) eigenvector for this value is equivalent to an acoustic mode eigenvalue. This could either be due to zero piezoelectric and piezomagnetic coefficient coupling for the mode in question or due to an exact canceling of the piezoelectric and piezomagnetic coupling (i.e., $\overline{\overline{d}}^T \overline{E}^i + \overline{\overline{q}}^T \overline{H}^i = \overline{0}$), where the electric and magnetic fields here are the eigenmodes associated with the eigenvalue. While the latter is theoretically possible it seems unlikely to occur unless the material is specifically engineered to have this property. Returning to the coupled magnetoelastoelectric problem, we proceed in a similar manner by substitution of Equation (12) into the constitutive Equation (2) (note this is not a reduced L assumption) to obtain

$$\overline{\overline{L}}\overline{\overline{T}} = \overline{\overline{d}}^T \overline{E} + \overline{\overline{q}}^T \overline{H}. \quad (17)$$

Eliminating displacement, \overline{u} , from the mechanical dynamics and small strain equations in (10) we see

$$\overline{\overline{S}} = ik\overline{\overline{N}}^T \left(-i\frac{k}{\rho\omega^2}\overline{\overline{N}} \right) \overline{\overline{T}} = \frac{1}{(\rho c^2)}\overline{\overline{N}}^T\overline{\overline{N}}\overline{\overline{T}}. \quad (18)$$

Further, assuming a strictly mechanical system where $\overline{\overline{S}} = \overline{\overline{s}}\overline{\overline{T}}$, we arrive at

$$\overline{\overline{s}}\overline{\overline{T}} = \frac{1}{(\rho c^2)}\overline{\overline{N}}^T\overline{\overline{N}}\overline{\overline{T}} \rightarrow \left(\frac{1}{(\rho c^2)}\overline{\overline{N}}^T\overline{\overline{N}} - \overline{\overline{s}} \right) \overline{\overline{T}} = \overline{0} \quad (19)$$

or equivalently $\overline{\overline{L}}\overline{\overline{T}} = \overline{0}$.

This defines the eigenvalue problem for a purely mechanical system. The eigenvalues of $\overline{\overline{L}}$ correspond to the phase velocities of the acoustic wave modes and are determined from the zeros of the characteristic polynomial for $\overline{\overline{L}}$, i.e., where the determinant $|\overline{\overline{L}}| = 0$. From consideration of this purely mechanical problem we see that the inverse of $\overline{\overline{L}}$ exists whenever the value of c^2 (actually values of ρc^2) is not an eigenvalue, or mechanical wave speed of the strictly mechanical system. Looking at Equation (13), we note that in the limit of $\overline{\overline{d}}$ and $\overline{\overline{q}}$ approaching zero, i.e., no electromagnetic cross-coupling, the purely mechanical eigenvalue problem is recovered as expected. This equation indicates how the mechanical wave is coupled into the electromagnetic wave. On physical grounds, when the right hand side of (13) is non-zero (i.e., so long as $\overline{\overline{d}}$ and $\overline{\overline{q}}$ are not identically zero), we would intuitively expect the phase velocities of the coupled waves to be different than the purely mechanical waves and consequently $\overline{\overline{L}}$ should be invertible for MEE wave modes. Consequently, we conclude that the matrix $\overline{\overline{L}}$ is invertible for the coupled system under analysis.

3.3. Calculation of $\overline{\overline{L}}^{-1}$

Noting that $\overline{\overline{L}}$ has the form $\frac{1}{\lambda}(\overline{\overline{A}} - \lambda\overline{\overline{B}})$ where $\lambda = \rho c^2$, $\overline{\overline{A}} = \overline{\overline{N}}^T\overline{\overline{N}}$ and $\overline{\overline{B}} = \overline{\overline{s}}$; we focus first on the form of the inverse for $(\overline{\overline{A}} - \lambda\overline{\overline{B}})$. On physical grounds, the compliance tensor $\overline{\overline{s}}$ is expected to be invertible;

the inverse being the material stiffness tensor. We assume that the eigenpairs are $\bar{\phi}_i$ and μ_i such that

$$\bar{A}\bar{\phi}_i = \mu_i \bar{B}\bar{\phi}_i \quad \text{or in matrix form} \quad \bar{A}\bar{\phi} = \bar{B}\bar{\phi}\bar{D} \quad (20)$$

with $\bar{\phi}$ the matrix of eigenvectors and \bar{D} the corresponding diagonal matrix of eigenvalues, μ_i . For convenience we further assume that the eigenvectors are normalized to unity. Since the matrix of eigenvectors is invertible we have

$$\bar{A} = \bar{B}\bar{\phi}\bar{D}\bar{\phi}^{-1}. \quad (21)$$

Now,

$$\bar{A} - \lambda\bar{B} = \bar{B}\bar{\phi}(\bar{D} - \lambda\bar{I}_6)\bar{\phi}^{-1} \quad (22)$$

and for $\lambda \neq \mu_i$,

$$(\bar{A} - \lambda\bar{B})^{-1} = \bar{\phi}(\bar{D} - \lambda\bar{I}_6)^{-1}\bar{\phi}^{-1}\bar{B}^{-1} \quad \rightarrow \quad \bar{L}^{-1} = \bar{\phi}\left(\frac{1}{\lambda}\bar{D} - \bar{I}_6\right)^{-1}\bar{\phi}^{-1}\bar{B}^{-1}. \quad (23)$$

Examining the diagonal matrix we find that

$$\begin{aligned} & \left(\frac{1}{\lambda}\bar{D} - \bar{I}_6\right)^{-1} \\ = - & \begin{bmatrix} \left(1 - \frac{\mu_1}{\lambda}\right)^{-1} & 0 & 0 & 0 & 0 & 0 \\ 0 & \left(1 - \frac{\mu_2}{\lambda}\right)^{-1} & 0 & 0 & 0 & 0 \\ 0 & 0 & \left(1 - \frac{\mu_3}{\lambda}\right)^{-1} & 0 & 0 & 0 \\ 0 & 0 & 0 & \left(1 - \frac{\mu_4}{\lambda}\right)^{-1} & 0 & 0 \\ 0 & 0 & 0 & 0 & \left(1 - \frac{\mu_5}{\lambda}\right)^{-1} & 0 \\ 0 & 0 & 0 & 0 & 0 & \left(1 - \frac{\mu_6}{\lambda}\right)^{-1} \end{bmatrix} \end{aligned} \quad (24)$$

When considering the predominately electromagnetic modes, the phase velocity (i.e., the eigenvalue associated with the electromagnetic wave speed) is generally much larger than the typical acoustic wave phase velocity. When $\mu_i = \rho c_a^2$ where c_a is one of the three possible acoustic velocities and $\lambda = \rho c^2$ is one of the five phase velocities for the magneto-electroelastic system. Assuming we select one of the two predominately electromagnetic modes, typically

$$\frac{\mu_i}{\lambda} = \left(\frac{c_a}{c}\right)^2 \ll 10^{-4}. \quad (25)$$

Consequently, $\frac{\mu_i}{\lambda} \ll 1$ and to very good approximation

$$\frac{1}{\left(1 - \frac{\mu_3}{\lambda}\right)} \approx 1 + \frac{\mu_3}{\lambda}. \quad (26)$$

With this approximation,

$$\left(\frac{1}{\lambda}\bar{D} - \bar{I}_6\right)^{-1} \approx -\bar{I} - \begin{bmatrix} \frac{\mu_1}{\lambda} & 0 & 0 & 0 & 0 & 0 \\ 0 & \frac{\mu_2}{\lambda} & 0 & 0 & 0 & 0 \\ 0 & 0 & \frac{\mu_3}{\lambda} & 0 & 0 & 0 \\ 0 & 0 & 0 & \frac{\mu_4}{\lambda} & 0 & 0 \\ 0 & 0 & 0 & 0 & \frac{\mu_5}{\lambda} & 0 \\ 0 & 0 & 0 & 0 & 0 & \frac{\mu_6}{\lambda} \end{bmatrix} = -\left(\bar{I} + \bar{\epsilon}\right) \quad (27)$$

where $\bar{\bar{\epsilon}}$ represents a diagonal matrix of small terms in $\frac{\mu_i}{\lambda}$. This implies

$$\bar{\bar{L}}^{-1} = -\bar{\bar{\phi}}(\bar{\bar{I}} + \bar{\bar{\epsilon}})\bar{\bar{\phi}}^{-1}\bar{\bar{B}}^{-1} = -\bar{\bar{B}}^{-1} - \bar{\bar{\phi}}\bar{\bar{\epsilon}}\bar{\bar{\phi}}^{-1}\bar{\bar{B}}^{-1} = -s^{-1} - \bar{\bar{\phi}}\bar{\bar{\epsilon}}\bar{\bar{\phi}}^{-1}\bar{\bar{s}}^{-1}. \quad (28)$$

For many MEE materials the second term has an impact of less than 1% and so L^{-1} can be conveniently replaced by $-s^{-1}$. In some MEE materials, or for specific directions within an MEE material, the EM phase velocities could be reduced by four or more orders of magnitude. Under these circumstances the higher order effect of the second term should not be ignored. The same is true when considering predominately acoustic modes. In these situations it is generally as easy to use the exact inverse given by Equations (23) and (24).

In the reduced MEE system, the effective tensor properties are functions of the phase velocity through their dependence on $\bar{\bar{L}}(c)$. Consequently this implicit system does not in general yield analytic solutions for phase velocity since the characteristic polynomial can be of 10th order, requiring numerical solution for the roots. Alternatively, the phase velocities can be found by iterative methods by assuming an initial value for the phase velocity, calculating a fixed estimate of $\bar{\bar{L}}$ and using this to calculate the effective parameters and eigenvalues of the system. Theoretically, this can be iterated to desired accuracy.

It is interesting to note that the $\bar{\bar{L}}$ matrix is 6×6 and would generally admit 6 eigenvalues, or wave speeds and the matched eigenmodes. It is well known that mechanical systems admit 3 eigenmodes, two shear and one longitudinal (in the same fashion that EM systems typically comprise two shear modes of propagation). It can be shown that 3 of the eigenmodes for $\bar{\bar{L}}$ correspond to the normal shear/longitudinal acoustic modes while the other 3 eigenvalues are zero. The zero modes correspond to static, $\omega = 0$, modes and do not relate to the predominately electromagnetic modes of interest in this article.

4. RESULTS

In this section we focus on the discussion of the electromagnetic modes of propagation rather than the acoustic modes even though both are present in our formulation. We noted above that $\bar{\bar{L}}$ looks like a perturbation of the negative compliance matrix for typical cases. In the limit of large c (phase velocity), the directional term in $\bar{\bar{L}}$, i.e., $\frac{1}{\rho c^2} \bar{\bar{N}}^T \bar{\bar{N}}$ has negligible effect on compliance and the inverse of $\bar{\bar{L}}$ is approximately $-\bar{\bar{s}}^{-1} = -\bar{\bar{c}}$, Equation (28), the negative inverse of the mechanical compliance tensor. In light of this, we can view each of the effective electromagnetic parameters as being the “usual” parameter modified by a stiffness coupling term. For example, the dielectric tensor $\epsilon_{eff} = \epsilon + \bar{\bar{d}}L^{-1}d^T$ consists of the material permittivity plus a piezoelectric “stiffening” term. We can see the effects of these stiffening factors by plotting the relative phase velocity of each mode as a function of direction in space (i.e., plot the parametric surface $(\theta, \phi, \frac{c}{c_0})$ where c is the phase velocity, c_0 is the speed of light in vacuum and θ, ϕ specify the direction of wave propagation).

Figure 1 shows a relative velocity profile for a LeadMgNiobate and CoFerrite composite with a 61% volume fraction of LeadMgNiobate. It is assumed that the ferroelectric and magnetic phases are polled along the x -direction. This produces strong anisotropy in the material. The material parameters for LeadMgNiobate and CoFerrite are listed in Table 1. Material properties for the composite LeadMgNiobate/CoFerrite were calculated by homogenizing the properties of a 2-2 connected, i.e., layered, structure. The composite properties for the LeadMgNiobate/CoFerrite are listed in Table 2.

The MEE material parameters for compliance, piezoelectric, piezomagnetic, permittivity, magnetoelectric and permeability tensors are estimated from the homogenization of a ferroelectric and ferromagnetic phase. The homogenization model assumes layered materials that are stacked in the z -direction. The polling of the piezoelectric and piezomagnetic phases are along the x -axis. For composites operating at higher frequencies the dynamic values of the materials are expected to be different but are presently unavailable. The effects of the stress-strain on the resultant values however, will still be significant.

For the LeadMgNiobate and CoFerrite material, the Mode 1 phase velocity in the plot with stress effects, Figure 2, is about 39% higher on the bulbous ends compared with the plot without stress effects,

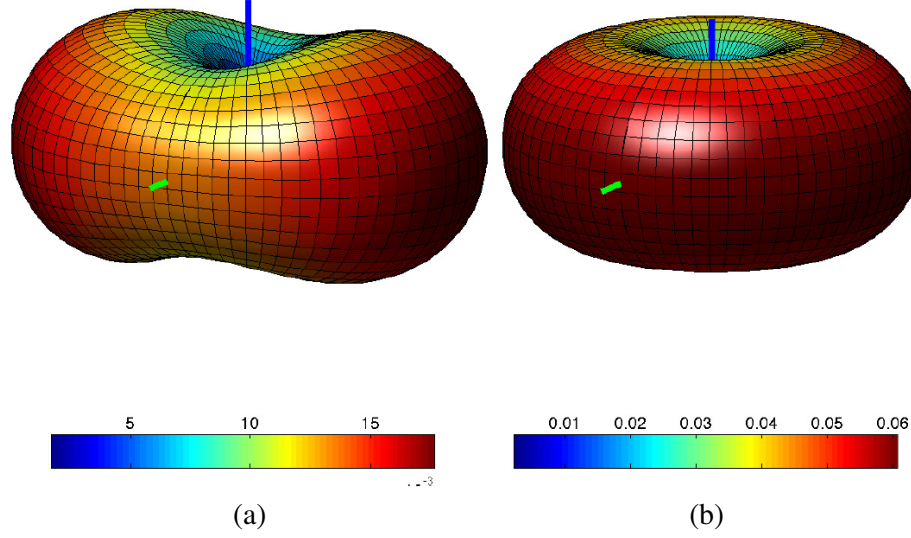


Figure 1. Phase Velocity Lead Magnesium Niobate (X Polled) — Cobalt Ferrite (X Polled). Relative phase velocity for the (a) Mode 1 and (b) Mode 2 propagating electromagnetic modes. These modes do not include the effects of strain-coupling in the material. The phase velocity range of Mode 1 is 0.0016804 to 0.017661. The phase velocity range of Mode 2 is 0.0022018 to 0.060663.

Table 1. Material data used for LeadMgNiobate-CoFerrite MEE material.

s_{11} [m ² /N]	s_{33}	s_{12}	s_{44}	s_{66}	
1.032×10^{-11}	1.199×10^{-11}	-3.1×10^{-12}	3.628×10^{-11}	2.257×10^{-11}	
e_{11}/e_0	e_{22}/e_0	e_{33}/e_0	μ_{11}/μ_0	μ_{22}/μ_0	μ_{33}/μ_0
1968.6	3375.88	2.25887	104.804	104.883	1.59155
d_{31} [pC/N]	d_{32}	d_{33}	d_{15}	d_{24}	
-0.1205	-0.1507	0.282	0.5063	0.0002	
q_{31} [m/A]	q_{32}	q_{33}		ξ_{11}	
0.0341×10^{-8}	0.0344×10^{-8}	-0.1154×10^{-8}		-3.151×10^{-8}	

Table 2. Materials properties Lead Magnesium Niobate-Metglas MEE material.

s_{11} [m ² /N]	s_{33}	s_{12}	s_{44}	s_{55}	s_{66}
1.221×10^{-11}	1.3×10^{-11}	-3.66×10^{-12}	2.651×10^{-11}	3.452×10^{-11}	3.174×10^{-11}
e_{11}/e_0	e_{22}/e_0	e_{33}/e_0	μ_{11}/μ_0	μ_{22}/μ_0	μ_{33}/μ_0
2560.42	1925.68	2.25887	479.454	774.05	17.3479
d_{31} [pC/N]	d_{32}	d_{33}	d_{15}	d_{24}	
-0.1526	-0.1332	0.3116	0.3521	0.0002	
q_{31} [m/A]	q_{32}	q_{33}		ξ_{21}	
0.0	0.0257×10^{-8}	-0.235×10^{-8}		8.397×10^{-8}	

Figure 1. The velocity profiles for the second mode 2 are essentially unchanged. This behavior is not uncommon based on the configurations examined by the authors to date.

Looking at a more extreme example, Figure 3 shows the velocity profile of a LeadMgNiobate-Metglas composite without stress interaction effects and with stress interaction effects. These figures illustrate the dramatic changes in phase velocity that can occur due to strain loading the material. It is

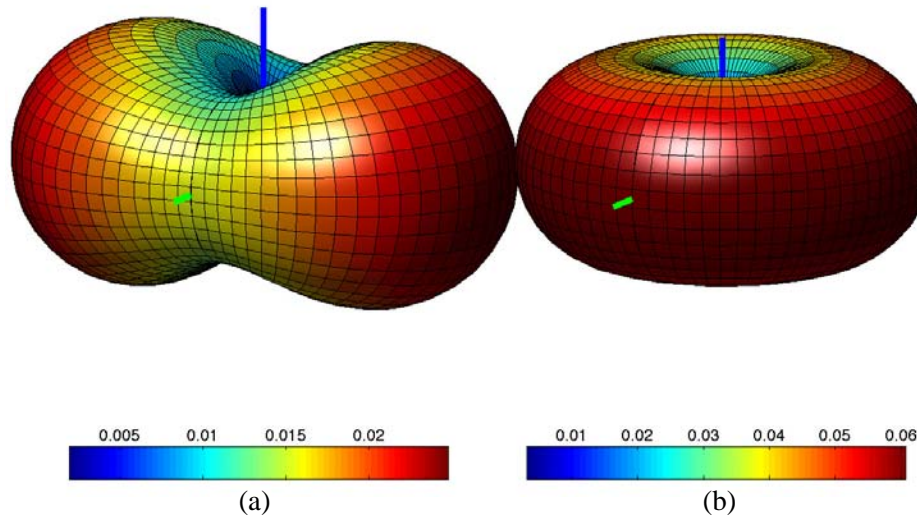


Figure 2. Phase Velocity Lead Magnesium Niobate (X Polled) — Cobalt Ferrite (X Polled). Relative phase velocity for the (a) Mode 1 and (b) Mode 2 propagating electromagnetic modes. These plots reflect the added “stiffening” terms in the respective permittivity, permeability and magntoelectric tensors. Note that the second mode is almost unaffected by change, while the velocity profile of the first mode is visually different. The phase velocity range of Mode 1 is 0.0019582 to 0.024752. The phase velocity range of Mode 2 is 0.0030843 to 0.06068.

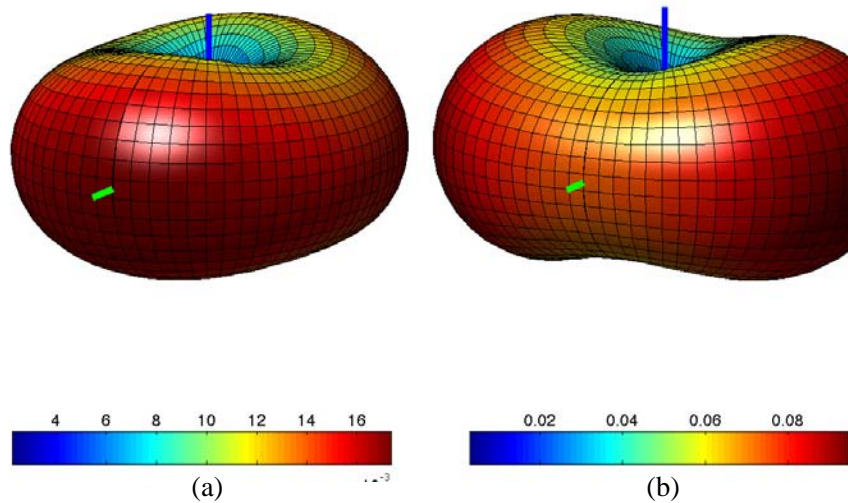


Figure 3. Phase Velocity Lead Magnesium Niobate (Y Polled) — Metglas (X Polled). Relative phase velocity for the (a) Mode 1 and (b) Mode 2 propagating electromagnetic modes. These modes do not include the effects of strain-coupling in the material. The phase velocity range of Mode 1 is 0.0022463 to 0.017345. The phase velocity range of Mode 2 is 0.0030396 to 0.094609.

interesting to note that the shifts in phase velocity can work in both directions (i.e., faster and slower) in a single propagation mode, see for example Figure 4 Mode 2, or leave a mode almost unaffected, Figure 2 Mode 2. As a homogenization model, the effective coefficients suggest how materials can be created with unusual properties not generally occurring in single phase materials.

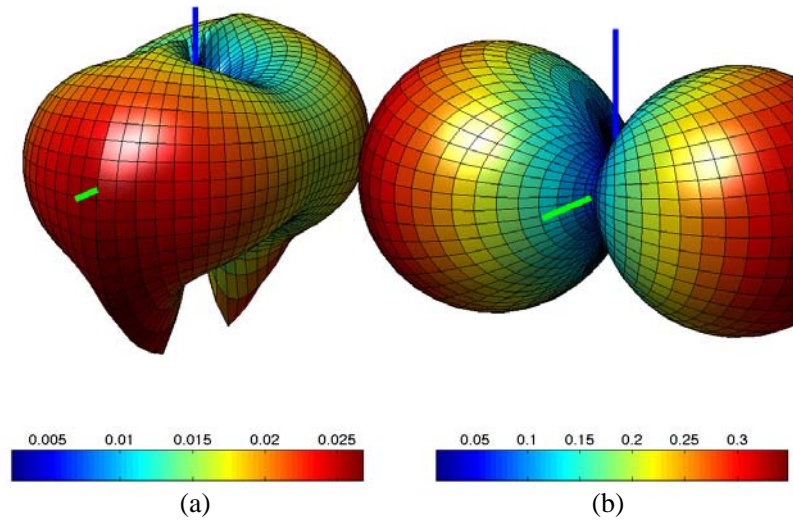


Figure 4. Phase Velocity Lead Magnesium Niobate (Y Polled) — Metglas (X Polled). Relative phase velocity for the (a) Mode 1 and (b) Mode 2 propagating electromagnetic modes. These plots reflect the added “stiffening” terms in the respective permittivity, permeability and magnetolectric tensors. Note that the second mode is visually different from the first mode. The phase velocity range of Mode 2 is

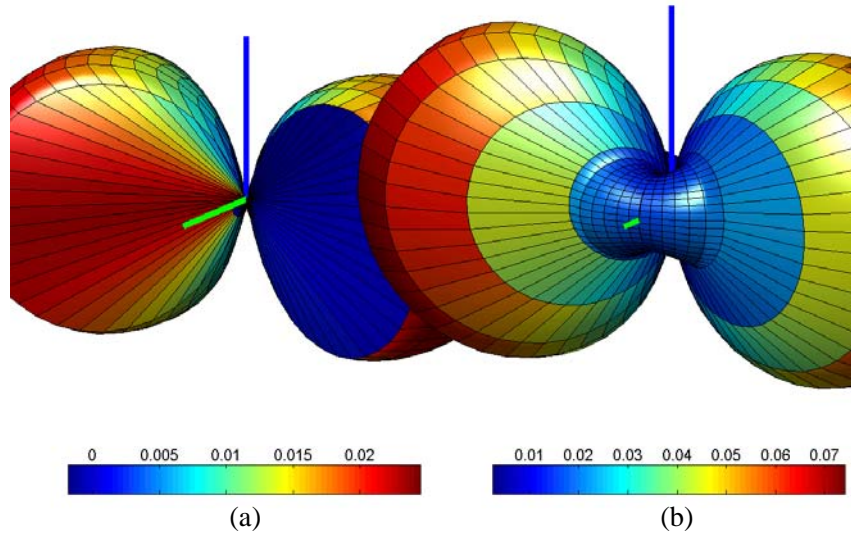


Figure 5. Showing modes with estimated strain. Note the apparent singularity on the first (right hand side) mode. For extreme material cases where the phase velocity is reduced several orders of magnitude the L inverse estimate is not effective. In the central region acoustic modes are found rather than the intended EM mode. The second mode reproduces correctly from the approximation.

An interesting property to note, however, is that as the material’s electromagnetic mode phase velocity drops, due to permittivity or permeable loading for example, see Figure 5, an effective directional compliance factor can become significant in $\bar{\bar{L}}$ and consequently feeds back into the other electromagnetic material parameters as well. In these extreme cases, the electromagnetic phase velocity becomes too close to the acoustic phase velocities and the $\bar{\bar{L}}$ tensor becomes ill-conditioned. In these cases, iteration to determine the phase velocity becomes un-stable.

5. CONCLUSIONS

By applying the mechanical equations of motion and small strain equations to the MEE constitutive relations, we derived an eigenvalue problem that can be solved for the appropriate phase velocities and eigenmodes. For high frequency ME applications this provides an effective solution of the coupled mechanical, electromagnetic MEE system. The effective parameters given yield reasonable values to treat systems as homogeneous magnetoelectric materials for typical applications. We find that the results obtained from our system including stress interaction effects are significantly different from those obtained from solutions which use only the permittivity, permeability and magnetoelectric coupling tensors. Further, we have shown that homogenized MEE materials can produce significant wave propagation effects not normally found in single phase materials.

ACKNOWLEDGMENT

This work was supported by the Air Force Office of Scientific Research (AFOSR) under grant No. FA9550-09-1-0677 managed by Byung-Lip (Les) Lee. The authors would also like to thank the NSF Nanosystems Engineering Research Center for Translational Applications of Nanoscale Multiferroic Systems (TANMS) Cooperative Agreement Award (No. EEC-1160504).

REFERENCES

1. Landau, L. and E. Lifshitz, *Electrodynamics of Continuous Medium*, Gostechizdat, Moscow, 1957.
2. Astrov, D. N., "The magnetoelectric effect in antiferromagnetics," *Soviet Physics JETP-USSR*, Vol. 11, No. 3, 708–709, 1960.
3. Fiebig, M., "Revival of the magnetoelectric effect," *Journal of Physics D: Applied Physics*, Vol. 38, R123–R152, Apr. 2005.
4. Ryu, J., S. Priya, K. Uchino, and H.-E. Kim, "Magnetoelectric effect in composites of magnetostrictive and piezoelectric materials," *Journal of Electroceramics*, Vol. 8, No. 2, 107–119, 2002.
5. Fetisov, Y. K. and G. Srinivasan, "Ferritepiezoelectric microwave phase shifter: Studies on electric field tunability," *Electronics Letters*, Vol. 41, No. 19, 1066, 2005.
6. Srinivasan, G., "Ferrite-piezoelectric layered structures: Microwave magnetoelectric effects and electric field tunable devices," *Ferroelectrics*, Vol. 342, 65–71, Oct. 2006.
7. Zhai, J., Z. Xing, S. Dong, J. Li, and D. Viehland, "Magnetoelectric laminate composites: An overview," *Journal of the American Ceramic Society*, Vol. 91, 351–358, Feb. 2008.
8. Chen, J. Y., H. L. Chen, and E. Pan, "Reflection and transmission coefficients of plane waves in magneto-electroelastic layered structures," *Journal of Vibration and Acoustics*, Vol. 130, 031002, Jun. 2008.
9. Iadonisi, G., C. Perroni, G. Cantele, and D. Ninno, "Propagation of acoustic and electromagnetic waves in piezoelectric, piezomagnetic, and magnetoelectric materials with tetragonal and hexagonal symmetry," *Physical Review B*, Vol. 80, 094103, Sep. 2009.
10. Yang, G.-M., X. Xing, A. Daigle, M. Liu, O. Obi, S. Stoute, K. Naishadham, and N. X. Sun, "Tunable miniaturized patch antennas with self-biased multilayer magnetic films," *IEEE Transactions on Antennas and Propagation*, Vol. 57, No. 7, 2190–2193, 2009.
11. Keller, S. M. and G. P. Carman, "Electromagnetic wave propagation in (bianisotropic) magnetoelectric materials," *Journal of Intelligent Material Systems and Structures*, Vol. 24, 651–668, Mar. 2013.
12. Pang, Y., J. Liu, Y. Wang, and D. Fang, "Wave propagation in piezoelectric/piezomagnetic layered periodic composites," *Acta Mechanica Solida Sinica*, Vol. 21, 483–490, 2008.
13. Chen, J., E. Pan, and H. Chen, "Wave propagation in magneto-electro-elastic multilayered plates," *International Journal of Solids and Structures*, Vol. 44, 1073–1085, 2007.

14. Wu, B., J. Yu, and C. He, "Wave propagation in non-homogeneous magneto-electro-elastic plates," *Journal of Sound and Vibration*, Vol. 317, 250–264, 2008.
15. Bichurin, M. I., V. M. Petrov, and G. Srinivasan, "Theory of low-frequency magnetoelectric effects in ferromagnetic-ferroelectric layered composites," *Journal of Applied Physics*, Vol. 92, No. 12, 7681–7683, Dec. 2002.
16. Chang, C. M., "Analytically evaluating the properties and performance of layered magnetoelectric composites," *Journal of Intelligent Material Systems and Structures*, Vol. 19, No. 11, 1271–1280, Apr. 2008.
17. Li, S., H. Du, Q. Xue, X. Gao, Y. Zhang, W. Shao, T. Nan, Z. Zhou, and N. X. Sun, "Large E-field tunability of microwave ferromagnetic properties in $\text{Fe}_{59.3}\text{Co}_{28.0}\text{Hf}_{12.7}$ /PZN-PT multiferroic composites," *Journal of Applied Physics*, Vol. 115, No. 17, 723, May 2014.
18. Pan, D. A., Y. Bai, A. A. Volinsky, W. Y. Chu, and L. J. Qiao, "Giant magnetoelectric effect in Ni-lead zirconium titanate cylindrical structure," *Applied Physics Letters*, Vol. 92, No. 5, 052904–3, 2008.
19. Ustinov, A. B., B. A. Kalinikos, and G. Srinivasan, "Nonlinear multiferroic phase shifters for microwave frequencies," *Appl. Phys. Lett.*, Vol. 104, No. 5, 052911, Feb. 2014.
20. Wan, J. G., J. M. Liu, H. L. W. Chand, C. L. Choy, G. H. Wang, and C. W. Nan, "Giant magnetoelectric effect of a hybrid of magnetostrictive and piezoelectric composites," *Journal of Applied Physics*, Vol. 93, No. 12, 9916–5, 2003.
21. Wang, X., E. Pan, J. D. Albrecht, and W. J. Feng, "Effective properties of multilayered functionally graded multiferroic composites," *Composite Structures*, Vol. 87, No. 3, 206–214, Feb. 2009.